# Motion Planning using Potential Fields for Robotic Image-Guided Intervention Systems

Mark Renfrew, Zhuofu Bai, M. Cenk Cavusoglu

***Abstract*— We present a simple approach to the problem of planning a needle's path during insertion in tissue. Then needle's motion is governed by nonholonomic constraints and by a requirement to avoid obstacles. We implement a motion planner that uses nonholonomic constraints to modify the commands given by an incremental holonomic planner, by satisfying the commands as closely as possible given the nonholonomic constrainsts. Additionally, our model uses only local information, making it suitable for image-guided needle insertions in which the locations of targets and obstacles is uncertain. We present experiments showing the effect of tuning the model's parameters, and we demonstrate two- and three-dimensional versions of the model.**

## I. Introduction

Physicians commonly perform needle insertion procedures for diagnostic or therapeutic purposes, such as biopsy or drug delivery. In these procedures, the needle must be inserted in such a way that the needletip intersects a target of interest, such as a tumor. The needle must also avoid obstacles, for example arteries or nerves.

DiMaio *et al.* [2] first proposed steering flexible needles from the needle base to the target, without touching obstacles or critical areas inside soft tissue. DiMaio and Salcudean captured deformations that happen during needle insertion into a gel and they simulated the insertion of needle using a quasi-static finite element method with measured tissue phantom parameters [3]. DiMaio and Salcudean [4] formulated a needle manipulation Jacobian using numerical needle deflection and soft tissue deformation models. In both simulation and experiments, they were able to steer needles to the target in the presence of obstacles by manipulating the needle base in soft tissue.

Webster *et al.* [5], proposed a kinematic model that describe the trajectory of flexible bevel-tip needles in rigid tissue. Parameters were fit using experimental data. Their model did not consider the interaction of the needle with an elastic medium. Reachability is a critical issue involved in this approach. Misra et al. [6] present a two dimensional model for a bevel tip needle embedded in an elastic medium. Their mechanics based model is based on both microscopic and macroscopic observations of the needle interaction with soft gels.

Park *et al.* [7] demonstrate a nonholonomic kinematic model to describe how an ideal needle with bevel tip moves through firm tissue with a numerical example. The reachability criteria are proven for this model, and an inverse kinematics method based on the propagation of needle-tip pose probabilities is presented.

We base our approach on that of De Luca and Oriolo [1]. They apply a potential field motion planner to a mobile robot which is subject to nonholonomic motion constraints.

Mark Renfrew (mxr90@case.edu) and Zhuofu Bai (zxb31@case.edu)are with the Department of Electrical Engineering and Computer Science, Case Western Reserve University, Cleveland, OH.

M. Cenk Çavuşoğlu (cavusoglu@case.edu) is an Associate Professor in the Department of Electrical Engineering and Computer Science, Case Western Reserve University, Cleveland, OH.

## II. Methods

If we denote the needletip's coordinates as $X, X \in \mathbb{R}^n$, we can specify its nonholonomic constraints by a matrix $A$ such that

$$A(X)\dot{X} = 0 \tag{1}$$

. All feasible velocities for the needletip must satisfy its kinematic model:

$$\dot{X} = G(X)u \tag{2}$$

where $G(X)$ forms a basis for the null space of $A(X)$.

Let $X_d(t)$ denote the desired trajectory of the robot at time $t$. We can obtain a valid input command $u$ (i.e., one that satisfies the nonholonomic constraints) by using pseudoinversion to minimize the error $\dot{X}_d - \dot{X}$ by least squares.

$$u = G^{\#}(X)\dot{X}_d = [G^T(X)G(X)]^{-1}G^T(X)\dot{X}_d \tag{3}$$

Note that if the desired robot velocity $\dot{X}$ satisfies the nonholonomic constraints, the error will be zero.

In our approach, we obtain our desired velocity $\dot{X}_d$ by using an incremental nonholonomic planner; specifically, an artificial potentials model. If we denote attractive and repulsive potentials by $U_a(X)$ and $U_r(X)$,

respectively, we obtain the desired velocity

$$\dot{X}_d = -\nabla_\chi U(X) = -\nabla_\chi (U_a(X) + U_r(X)) \quad (4)$$

.

We use a simple linear/quadratic model for the attractive potential. That is, the force is a linear function when the needletip is far from the target, and a quadratic function when near:

$$U_a(X) = \begin{cases} \zeta ||X - X_{goal}|| & , ||X - X_{goal}|| \leq d* \\ \frac{1}{2}\zeta ||X - X_{goal}||^2 & , otherwise \end{cases} \quad (5)$$

, where $X_{goal}$ is the goal position, $X$ is the needletip position, $d*$ is a parameter specifying the distance from the goal at which the function changes, and $\zeta$ is a parameter governing the strength of the field.

We calculate the repulsive field as follows:

$$U_r(X) = \begin{cases} \frac{1}{2}\eta(\frac{1}{||X - X_{obs}||} - \frac{1}{Q*})^2 & , ||X - X_{obs}|| \leq Q* \\ 0 & , otherwise \end{cases} \quad (6)$$

,

where $Q*$ is a parameter governing the effective distance of the repulsive field and $\eta$ governs its strength.

### A. Kinematic Models

We formulated kinematic models for both the 2-dimensional and 3-dimensional cases.

*1) Two-Dimensional Case:* In the 2-D case, the non-holonomic constraints are expressed as

$$\begin{bmatrix} sin\theta & -cos\theta & 0 \end{bmatrix} \begin{bmatrix} \dot{x} \\ \dot{y} \\ \dot{\theta} \end{bmatrix} \quad (7)$$

, and the kinematic model specified by

$$\begin{aligned} \dot{x} &= cos\theta u_1 \\ \dot{y} &= sin\theta u_1 \\ \dot{\theta} &= u_2 \end{aligned} \quad (8)$$

where $u_1$ is the needle's forward velocity and $u_2$ is its turning velocity. The control input $u$ is given by

$$u = G^{\#}(X)\dot{X}_d = \begin{bmatrix} cos\theta & sin\theta & 0 \\ 0 & 0 & 1 \end{bmatrix} \begin{bmatrix} \dot{x_d} \\ \dot{y_d} \\ \dot{\theta_d} \end{bmatrix} \quad (9)$$

.

To enforce unicycle-like motion, we choose the desired angle using

$$\dot{\theta_d} = atan2(\dot{x_d}, \dot{y_d}) - \theta \quad (10)$$

, which leads to the following equations for the velocities of the needletip:

$$\begin{aligned} u1 &= k_p(\dot{x_d}cos\theta + \dot{y_d}sin\theta) \\ u2 &= k_\theta(atan2(\dot{x_d}, \dot{y_d}) - \theta) \end{aligned} \quad (11)$$

, where $k_p$ and $k_\theta$ are used to scale the turning and driving velocities, e.g., to make the needle stiffer or less stiff.

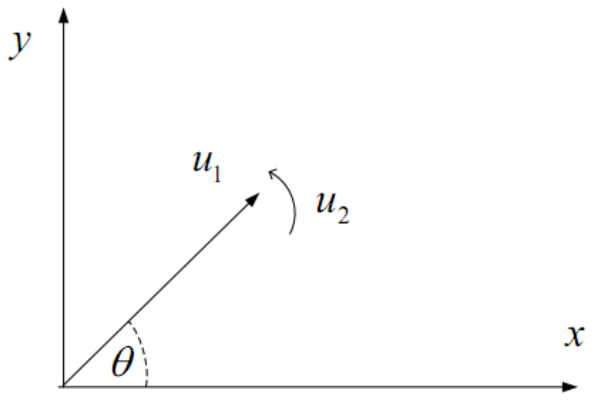


Fig. 1. Diagram showing the physical meaning of terms in the 2-D model.

*2) Three-Dimensional Case:* In the 3-D case, the kinematic model becomes

$$\begin{aligned} u_3 &= u_1 cos\phi \\ \dot{x} &= u_3 cos\theta = u_1 cos\phi cos\theta \\ \dot{y} &= u_3 sin\theta = u_1 cos\phi sin\theta \\ \dot{z} &= u_1 sin\phi \\ \dot{\theta} &= u_2 \\ \dot{\phi} &= u_4 \\ u_1 &= k_p[(\dot{x_d}cos\theta + \dot{y_d}sin\theta)cos\phi + \dot{z_d}sin\phi] \\ u_2 &= k_\theta(atan2(\dot{y_d}, \dot{x_d}) - \theta)) \\ u_4 &= k_\phi(atan2(\dot{z_d}, \sqrt{\dot{x_d^2} + \dot{y_d^2}}) - \phi) \end{aligned} \quad (12)$$

. This formulation is similar to the 2-D one, with the addition of a $\phi$ term to account for the angle above the x-y plane, and a $u_4$ term to account for the second turning velocity.

## III. Simulation Results

In order to determine parameter values to make We first performed experiments using the 2-D formulation, for simplicity. In all experiments, we vary $k_\theta$ while holding the remaining parameters constant. We also hold the needle's initial direction to be pointing toward the

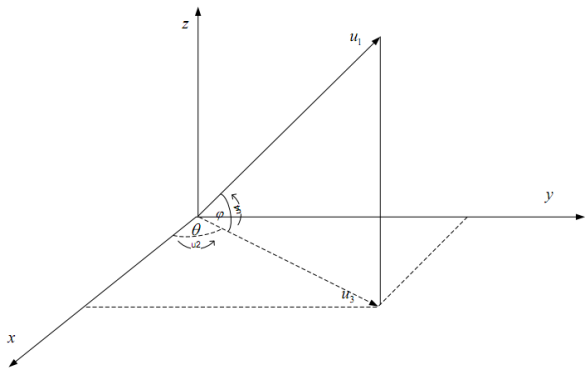


Fig. 2. Diagram showing the physical meaning of terms in the 3-D model.

goal for all experiments.

$$Q* = 20$$
$$d* = 5$$
$$\zeta = 1$$
$$\eta = 1000$$
$$k_p = 1$$

In all experiments, the start position is at (0,0) and the goal position at (100, 100). Obstacles are placed at various positions.

In the first experiments, we place an obstacle at (60,70) and observe the effect that varying the turning speed has.

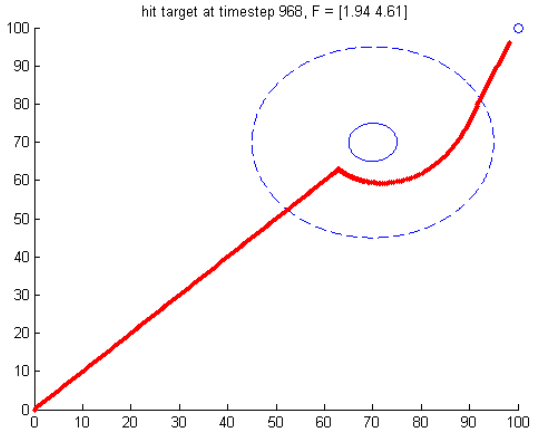


Fig. 3. Experiment 1;$k_\theta = 1$.

We see that a value for $k_\theta$ that is too low will cause the needle to be unable to hit the target, while a value that is too high will cause it to move in ways that a real needle would be unable to. Choosing $k_\theta = 0.1$, we

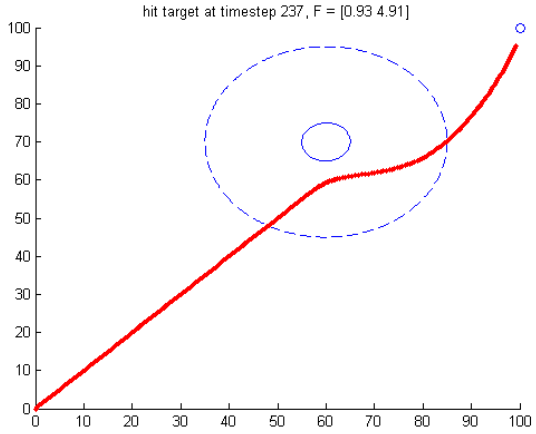


Fig. 4. Experiment 1;$k_\theta = 0.1$.

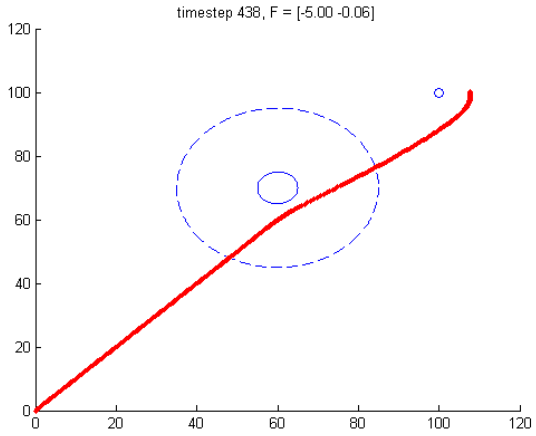


Fig. 5. Experiment 1;$k_\theta = 0.01$.

see that the needle is able to navigate relatively complex environments with more obstacles.

The model is also able to navigate relatively complex environments in 3 dimensions.

## IV. Discussion and Conclusion

We have adapted the nonholonomic motion planning approach of De Luca and Oriolo to simulate the motion of a needle inside tissue. Given appropriate parameters, the model can adequately simulate a needle's motion. However, given inappropriate parameters, the planned motion does not resemble a path that is possible for a needle. Additionally, we have only guessed at parameters, rather than doing any experiments to determine reasonable values for a needle's nonholonomic constraints. Furthermore, this model assumes that a needletip moves

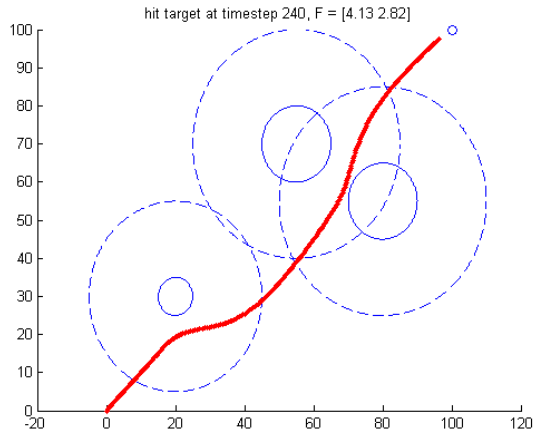


Fig. 6. Experiment 2;$k_\theta = 1$.

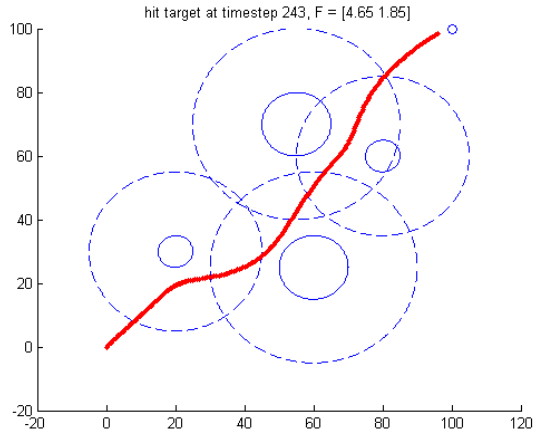


Fig. 7. Experiment 2;$k_\theta = 1$.

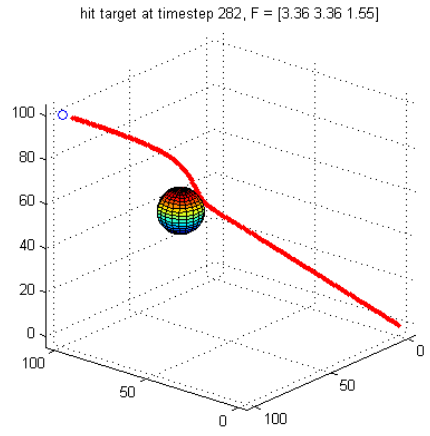


Fig. 8. Experiment 3;$k_\theta = 1$.

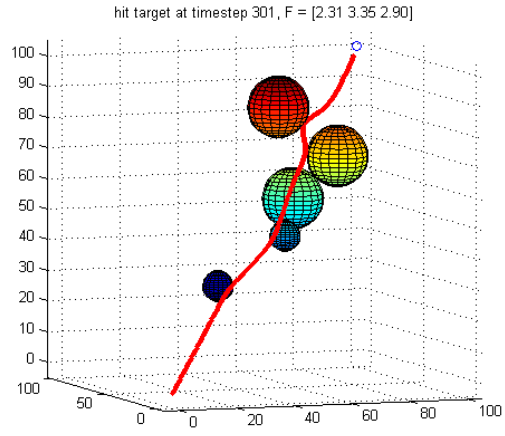


Fig. 9. Experiment 3;$k_\theta = 1$.

independently of the needle body, when in fact a change in the needletip direction is the result of a larger change in the configuration of the needle. A more sophisticated model of the nonholonomic constraints must be developed to address this.

## REFERENCES


[1] A. De Luca and G. Oriolo. Local incremental planning for nonholonomic mobile robots. In *Robotics and Automation, 1994. Proceedings., 1994 IEEE International Conference on*, pages 104–110. IEEE, 1994.

[2] Simon P. DiMaio. *Modelling, simulation and planning of needle motion in soft tissue*. Ph.d., University of British Columbia, Vancouver, Canada, 2003.

[3] S.P. DiMaio and S.E. Salcudean. Needle insertion modeling and simulation. *Robotics and Automation, IEEE Transactions on*, 19(5):864 – 875, 2003.

[4] S.P. DiMaio and S.E. Salcudean. Needle steering and motion planning in soft tissues. *Biomedical Engineering, IEEE Transactions on*, 52(6):965 –974, 2005.

[5] R. J. Webster III, J. S. Kim, N. J. Cowan, G. S. Chirikjian, and A. M. Okamura. Nonholonomic modeling of needle steering. *International Journal of Robotics Research*, 25(5-6):509–525, May-June 2006.

[6] S. Misra, K.B. Reed, B.W. Schafer, K.T. Ramesh, and A.M. Okamura. Observations and models for needle-tissue interactions. In *Robotics and Automation, 2009. ICRA '09. IEEE International Conference on*, pages 2687–2692, May 2009.

[7] Wooram Park, Jin Seob Kim, Yu Zhou, N.J. Cowan, A.M. Okamura, and G.S. Chirikjian. Diffusion-based motion planning for a nonholonomic flexible needle model. In *Robotics and Automation, 2005. ICRA 2005. Proceedings of the 2005 IEEE International Conference on*, pages 4600–4605, 2005.